Changing depositional environments in the Colombian Fúquene Basin at submillennial time-scales during 284-27 ka from unmixed grain-size distributions and aquatic pollen

M. Vriend[1], M.H.M. Groot[1], H. Hooghiemstra[1,*], R.G. Bogotá-Angel[1,2] & J.C. Berrio[1,3]

1 Institute for Biodiversity and Ecosystems Dynamics (IBED), University of Amsterdam, Science Park 904, 1098 XH Amsterdam, the Netherlands.

2 Facultad del Medio Ambiente y Recursos Naturales. Universidad Distrital Francisco José de Caldas, Bogotá, Colombia.

3 Present address: Department of Geography, University of Leicester, U.K.

* Corresponding author. Email: h.hooghiemstra@uva.nl.

Abstract

In a ~60 m long record reflecting the period from 284 ka to 27 ka we analysed grain size distributions (GSD), organic carbon content, and aquatic pollen assemblages at 1-cm increments. The 4768-points time series show with ~60 yr resolution the dynamic history of Lake Fúquene (2540 m alt., 4° N lat.) of the northern Andes during two full interglacial-glacial cycles. GSD show proportions of clay, fine silt, coarse silt, and sand evidencing the location of the sediment source (proximal vs distal) in relation to the drilling site, and available energy to transport sediments in the catchment area. Loss-on-ignition (LOI) values reflect estimates of the abundance of organic matter (OM) in the sediments. Aquatic pollen were grouped into assemblages characteristic of deep water, shallow water, swamp, and wet lake shore environments, reflecting a hydrological gradient sensitive for lake level changes.

The End-Member Modelling Algorithm (EMMA) showed that 4 end-members (EMs) explain an optimal proportion (70%) of the observed variation. EMMA is able to unmix GSD of lacustrine sediments in a genetically meaningful way allowing EMs to be interpreted in past depositional and environmental settings. Most unexplained variability is located in the fraction of coarse sediment. OM content was estimated on the basis of LOI data and formed a fifth EM that mainly indicates presence of peat. Changes concur with submillennial-scale variability established in other proxies from this record (Groot et al., 2011). Periods with distinct sediment compositions are 284-243 ka (mainly MIS 8), 243-201 ka (mainly MIS 7), 201-179 ka (mainly MIS 7/6 transition), 179-133 ka (mainly MIS 6), 133-111 ka, (mainly MIS 5e) 111-87 ka (mainly MIS 5d-5b), 87-79 ka (mainly MIS 5a), 79-62 ka (mainly MIS 4), and 62-27 ka (MIS 3) showing sedimentological regimes are climate driven.

Keywords: depositional environments, Lake Fúquene, grain size distributions, End Member Modeling Algorithm, aquatic pollen

Introduction

The Fúquene Basin (2540 m elevation) is covered by Quaternary lacustrine sediments and at present-day only a part is covered by a lake. Previous palaeoecological studies from sediment cores collected at marginal sites of the lake have demonstrated that sediments represent a rich archive of vegetation and climate change. We refer to the pollen records Fúquene-2 (Van Geel & Van der Hammen, 1973), Fúquene-3 (Van der Hammen & Hooghiemstra, 2003) and composite core Fúquene-7C (Mommersteeg, 1998).

Erosion of the various rock formations in the catchment area (Sarmiento et al., 2008) and riverine transport of sediments produced a more than 60 m thick sediment sequence in the basin. The vegetation in the catchment area is the source of plant debris and organic matter (OM) which is transported by water currents to the lake. Pollen grains are mainly transported by wind to the lake sediments. Here we analyse in a sediment core the temporal changes in sediment composition in concert with the changes in aquatic vegetation and OM content. The granulometric composition of lacustrine sediments is mostly expressed by univariate grain-size

properties such as the mean or median grain size (Julià & Luque, 2006) or by sediment fractions (Burrough et al., 2007; Chapron et al., 2007). An alternative approach to interpret lacustrine sediments was used by Torres et al. (2005) for sediments of the adjacent Bogotá Basin. He distinguished eleven sedimentary facies on the basis of visual inspection of the grain size distributions (GSD). However, all these approaches neglect the common fact that sediments are mixtures of sediment populations derived from different sources, and that sediments have been transported to the site of deposition by different mechanisms (Weltje & Prins, 2003). Therefore, a meaningful genetic interpretation of lacustrine sediment sequences requires to unravel GSD in its elementary components.

Assuming that lacustrine sediments represent mixtures of sediment supplied by various transport processes – varying from clay settlement to turbidity currents – and from different sediment sources, bulk samples should be unmixed in its genetic components representing relative contributions of typical transport-deposition processes. Recent studies have indicated that unmixing of aeolian, fluvial, and marine sediments can be accomplished with the End-Member Modelling Algorithm (EMMA; Holz et al., 2004, 2007; Stuut & Lamy, 2004; Vriend & Prins, 2005; Prins et al., 2007; Prins & Vriend, 2007; Vriend et al., 2011). EMMA considers the measured GSD as a series of mixtures and allows estimation of the elementary sediment components and their proportional distributions in the analysed sediment samples (Weltje, 1997; Prins & Weltje, 1999a; Weltje & Prins, 2003, and references herein; Weltje & Prins, 2007). The palaeoenvironmental significance of GSD becomes evident if they can be expressed in terms of a mixing model with a limited number of sediment components, and each sediment component can be tied to a specific transport process and/or sediment source. Further information can be obtained by comparing the mixing model with the aquatic pollen record. Changes in the proportions of categories of aquatic pollen reflect a gradient from deep water to shallow water, swamp, and wet shore vegetation, indicating changes in the position of the shoreline relative to the drilling site. This signal reflects changes in water depth (Van 't Veer & Hooghiemstra, 2000; Torres et al., 2005). As the Fúquene Basin has a flat topography this signal rather reflects changes in lake size. The relationship between downcore proportions of end-members (EMs) and vegetation associations of the hydrosere across a lake border gives insight in the changing depositional environments.

Here we analyse the abiotic and the biotic signals in the ~60 m long sediment core Fúquene-9C (Fq-9C) which was analysed at 1-cm increments. The core reflects the period from 284 ka to 27 ka and changes are shown with ~60 yr temporal resolution (Groot et al., 2011). Compared to the study of the downcore grain size analysis in the adjacent Bogotá Basin (Torres et al., 2005), we improved the methodological approach substantially. This paper presents the unmixing results obtained from sediment populations in the GSD as EMs. We interpreted these modelled sediment components into plausible sediment transport processes and depositional environments and reconstructions are embedded in records of local and regional vegetation change.

Environmental setting

Lake Fúquene (5°27' N, 73°46' W) is located at 2540 m elevation in the Eastern Cordillera of Colombia (Fig. 1). The surrounding mountains are up to 3200 m altitude covered by upper montane forest, between 3200 and 3500 m by subpáramo, and from 3500 m to the highest tops at 3700 m by grasspáramo (Van Geel & Van der Hammen, 1973; Van der Hammen, 1974; Van 't Veer & Hooghiemstra, 2000). The drainage basin covers ~1750 km² and extends between 5°35' N and 5°19' N, and between 73°54' W 73°35' W (IGAC, 2003). At present-day the lake surface is ~25 km² and water depth varies between 2 and 6 m. The lake covers a small part of the floor of the southern part of the basin (CAR, 2000; Santos-Molano & Guerra-C, 2000; Sarmiento et al., 2008). Field observations at several locations in the basin evidenced that lacustrine sediments occur up to ~20 m above the present-day lake level indicating that Lake Fúquene was during the time recorded not deeper than ~25 m for a significant period of time. As the topography of the basin floor is flat, small lake level changes have a large impact on the lake surface.

From a hydrological point of view Lake Fúquene is an open lake with inlets from the Ubaté River and several small streams in the south and east, and the Suarez River as the main outlet in the northwest (Fig. 1). At present only the southern part of the basin (~900 km²) is functioning as a catchment area for the lake; the northern part of the basin (ca 850 km²) is now covered by swamps and grasslands and precipitation from this part of the basin pours into the Suarez River and directly leaves the basin at the Saboya Dam (Sarmiento et al., 2008). The lake is predominantly underlain by sandstone of Cretaceous and Tertiary age (Ingeominas, 1991). Periodically the basin receives wind-blown volcanic ash from massive eruptions in the Central Cordillera (Riezebos, 1978). Only the finest ash fraction is found mixed up with lacustrine sediments.

The almost equatorial position of Lake Fúquene explains the climate of the study area is mainly influenced by the annual migration of the Inter-Tropical Convergence Zone (ITCZ). Two relatively dry seasons, from December to January and from July to August, alternate with two rainy seasons from February to June and September to November. The annual precipitation ranges from 1100 mm in the north up to 770 mm in the south where a rain shadow effect is evidenced by presence of cactaceous vegetation (CAR, 2002). The seasonal temperature cycle is weak with mean monthly temperatures of ~13.5±0.5° C. The daily temperature range is large and during the dry season night frost may occur (IGAC, 2003).
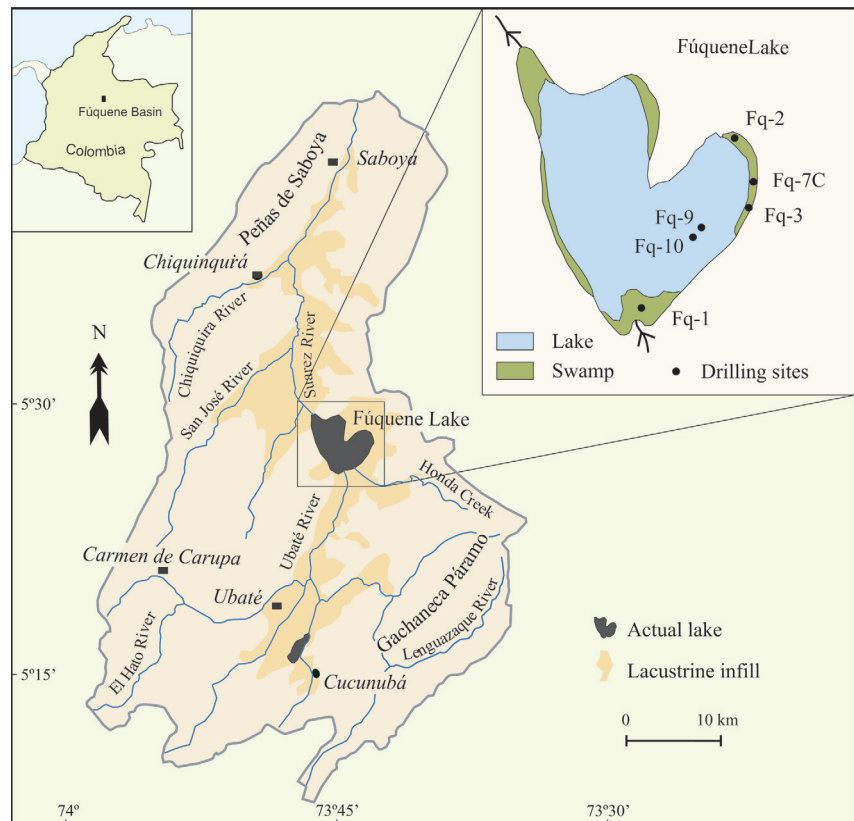
Fig. 1. Map showing the contour of the drainage area of the Fúquene Basin, the distribution of lacustrine sediments, the drainage system, and the size of present-day Lake Fúquene. The inset map shows the location of the cores mentioned in the text.

Materials and Methods

Chronology

Two parallel cores of ~60 m long were used to build the composite record Fúquene Basin Composite (Fq-BC) reaching >90% sediment recovery (Groot et al., 2011). The core was dated by radiocarbon ages, cyclostratigraphical analysis of the arboreal pollen percentage (AP%) record reflecting temperature change, and orbital tuning (Groot et al., 2011). Highly significant power at 22.65 and 9.07 m, respectively, reflect the imprint of the ~100 kyr glacial-interglacial cycle, and the 41 kyr obliquity cycle. The ~9 m period was filtered from the AP% record and tuned to the 41 kyr component filtered from the global $\partial^{18}O$ benthic stack record LR04 (Lisiecki & Raymo, 2005). The result is a tuned age model (Fig. 2) showing the sediment core reflects the period from ~27,000-284,000 years before present (~27-284 ka) (for more details see Groot et al., 2011). In between tie points (Fig. 2) sediment accumulation is assumed quasi linear but changes in GSD show sediment accumulation varied at millennial time scales. Here we reached the limits of chronological control.

Sediment collection and analysis

We generated data sets at 1 cm increments along the core, reflecting ~60 yr temporal resolution, for X-ray fluorescence (XRF) based geochemical analysis (a non-destructive procedure that determines the chemical composition of measured sediments as element intensities; see Jansen et al. (1998) and Bogotá-Angel et al., (2011a) for more details), loss-on-ignition (LOI) based OM content, pollen spectra, and grain size analysis. Grain size analysis was carried out at the Vrije Universiteit Amsterdam.
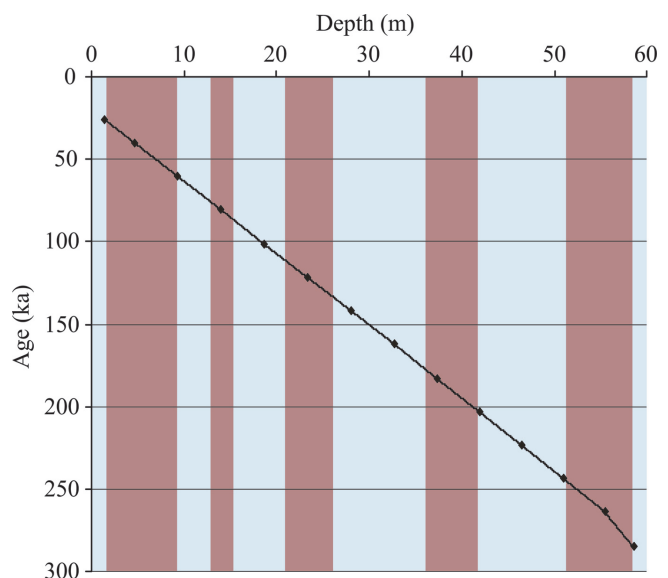

Fig. 2. Simplified depth versus age model of record Fq-9C. Results are taken from Groot et al. (2011) Diamonds reflect tie points of the tuning of the arboreal pollen percentage record to the global $\partial^{18}O$ benthic stack record LR04 (Lisiecki & Raymo, 2005). The nine discrete sediment sequences / periods with characteristic lacustrine sedimentary environments are shown.

GSD have been measured with a Fritsch Analysette 22 laser particle sizer, which results in a GSD with 56 size classes in the size range from 0.15 to 2000 μm. Prior to grain-size measurement, the samples were prepared according to the methods described by Konert & Vandenberghe (1997). About 1 to 2 g of bulk sediment was pre-treated with H_2O_2 and HCl to remove OM and carbonates, respectively. As a consequence, the results of the grain-size analysis reflect the GSD of the siliciclastic sediment fraction. Selected intervals also contain volcanic ash which originate from the Central Cordillera and has been wind blown to the Eastern Cordillera. Therefore only a fine grained ash fraction is available which is very dispersed in the sediment column by action of water current transport. Diatoms generally range in size from 10 to 150 μm and can be found in any marine or lacustrine environment (Wolin & Duthie, 1999). Diatom valves are made up of SiO_2 which is not affected by the normal sample preparation prior to grain-size measurement. Therefore high diatom percentages in sediments potentially can obscure the results of grain-size measurements. We evaluated the presence of diatoms in the sediments by analysing 30 random samples. Sample preparation followed a standard procedure (Battarbee, 1986). In 28 out of the 30 samples we found less than 1% diatoms. Only two samples contained diatoms, 10% and 40%, respectively.

Quantitative analysis of main elements was carried out for 30 samples using Inductively Coupled Plasma Mass Spectroscopy (ICP-MS). The $CaCO_3$ content was calculated using the Ca values with the assumption that all Ca is $CaCO_3$ derived. The amount of $CaCO_3$ of the sediment ranges from 0.3 to 1.5% with an average value of 0.6% Weight percent of OM in the sediment is determined by heating of sediment samples in a muffle furnace. After oven-drying of the sediment samples to constant weight (24 h at 105° C) OM is combusted to ash and carbon dioxide at a temperature of 375° C (16 h). Following Beaudoin (2003), we used a combustion temperature of 375° C to avoid loss of interstitial water from clays and the breakdown of carbonates. LOI values are calculated with:

$$LOI_{375} = ((DW_{105} - DW_{375}) / DW_{105}) \cdot 100$$

Where LOI_{375} (wt%) represents LOI at 375° C, DW_{105} (g) represents the dry weight of the sediment sample before combustion and DW_{375} (g) the dry weight of the sediment sample after heating to 375° C.

Decomposition of GSDs

Natural sediments show a large variability in distributional shapes as result of various processes active during transport and deposition (Prins & Weltje, 1999b; Weltje & Prins, 2007). Unmixing of grain-size data in a genetic meaningful way can be obtained by means of EMMA (Weltje, 1997). This modelling algorithm has been designed to provide the simplest possible explanation of the observed variation among a set of compositions (e.g. GSD) in absence of a-priori knowledge of the (geological) system under study. The EM modelling is required to decompose GSD into proportional contributions of an optimal set of EMs whose distributions are not restricted to a particular class. The method needs an array of GSD; it can not operate on a single GSD. The resulting mixing model is subject to strict non-negativity and constant-sum constrains on EM compositions and mixing coefficients to ensure physical interpretability of the modelling results (Weltje & Prins, 2003, 2007). The EM model solves the mixing problem in two stages. Stage one estimates the number of EMs. The minimum number of EMs required for a satisfactory approximation of the data is estimated by calculating the coefficient of determination (r^2). This represents the proportion of variance of each grain-size class which can be reproduced by the approximated data (Weltje, 1997). Experiments with synthetic mixtures of natural sediments have shown that the true number of EMs (n) corresponds to the value of n at the inflection point of the (n – mean r^2) curve (Prins & Weltje, 1999a). Stage two estimates the EM compositions and their mixing coefficients to the bulk sediment. The composition of the EMs encloses as many of the initial data points as tightly as possible (Weltje & Prins, 2007)

Vegetation based lake level fluctuations and temperature reconstructions

At the border of lakes plant species composition varies with water depth and the stability of the shore. Along such hydrological gradient a suite of plant species are indicative of the local depositional environment. In the northern Andes the ecological ranges of plants from aquatic and marsh environments was studied by e.g. Van der Hammen & González (1960), Cleef (1981), Rangel & Aguirre (1983, 1986), Cleef & Hooghiemstra (1984), Cortés & Rangel (2000), and Chaparro (2003). Cleef (1981) and Rangel (2003) have described the actual hydrosere and recognised different successional vegetation communities related to water depth. In the pollen spectra we identified the following categories: (a) shore indicator taxa: *Polygonum*, *Rumex*; (b) swamp indicator taxa: Cyperaceae; (c) shallow water indicator taxa: Apiaceae, *Hydrocotyle*, *Ludwigia*, *Myriophyllum*, Ranunculaceae, *Typha*; (d) deep water indicator taxa: *Isoëtes*, *Potamogeton* (see also Torres et al., 2005).

On a regional scale changes in the altitudinal vegetation distribution are mainly temperature driven (e.g. Van der Hammen, 1974; Van 't Veer & Hooghiemstra, 2000; Bogotá-Angel et al., 2011; Groot et al., 2011). The present-day upper forest line (UFL) is at ~3200 m and coincides with a mean annual temperature (MAT) of 9.5° C. Using a lapse rate of 0.6° C per 100 m UFL displacement past temperatures are calculated.

Pollen preparation, pollen analysis and zonation

Pollen samples were prepared following standard palynological preparation techniques (Feagri & Iversen, 1989) including sample treatment with sodium pyrophosphate, acetolysis, and heavy liquid separation by bromoform. Pollen samples were mounted in a glycerin gelatin medium. Pollen sum values range from 60 to 712 with a mean value of 350 grains. Pollen identification was based on Hooghiemstra (1984) and the pollen reference collection at the University of Amsterdam. Pollen analysis was carried out by a trained team of palynologists at University of Amsterdam and at the Universidad Nacional de Colombia in Bogotá. Zonation of the records was established on the basis of stratigraphical constrained cluster analysis using the total sum of squares (CONISS; Grimm, 1987; Gill et al., 1993).

Analysis and results

End members

The suite of GSD (n = 4768) was used as input data for EMMA. Summary statistics are calculated concerning the mean GSD and maximum range of volume frequencies of each grain-size class in the data set (Fig. 3a). The distribution of the coefficient of determination (r^2) is estimated for each grain-size class for the different mixing models with varying numbers of EMs (Fig. 3b). The mean coefficient of determination increases when the number of EMs is increased (Fig. 3c). The inflection point in the $n - r^2_{mean}$ curve lies at n = 4 ($r^2_{mean} = 0.7$) indicating that a four-EM mixing model reproduces on average 70% of the variance in the dataset. The r^2 data also indicates that the use of five, or more EMs hardly improves the goodness-of-fit statistics
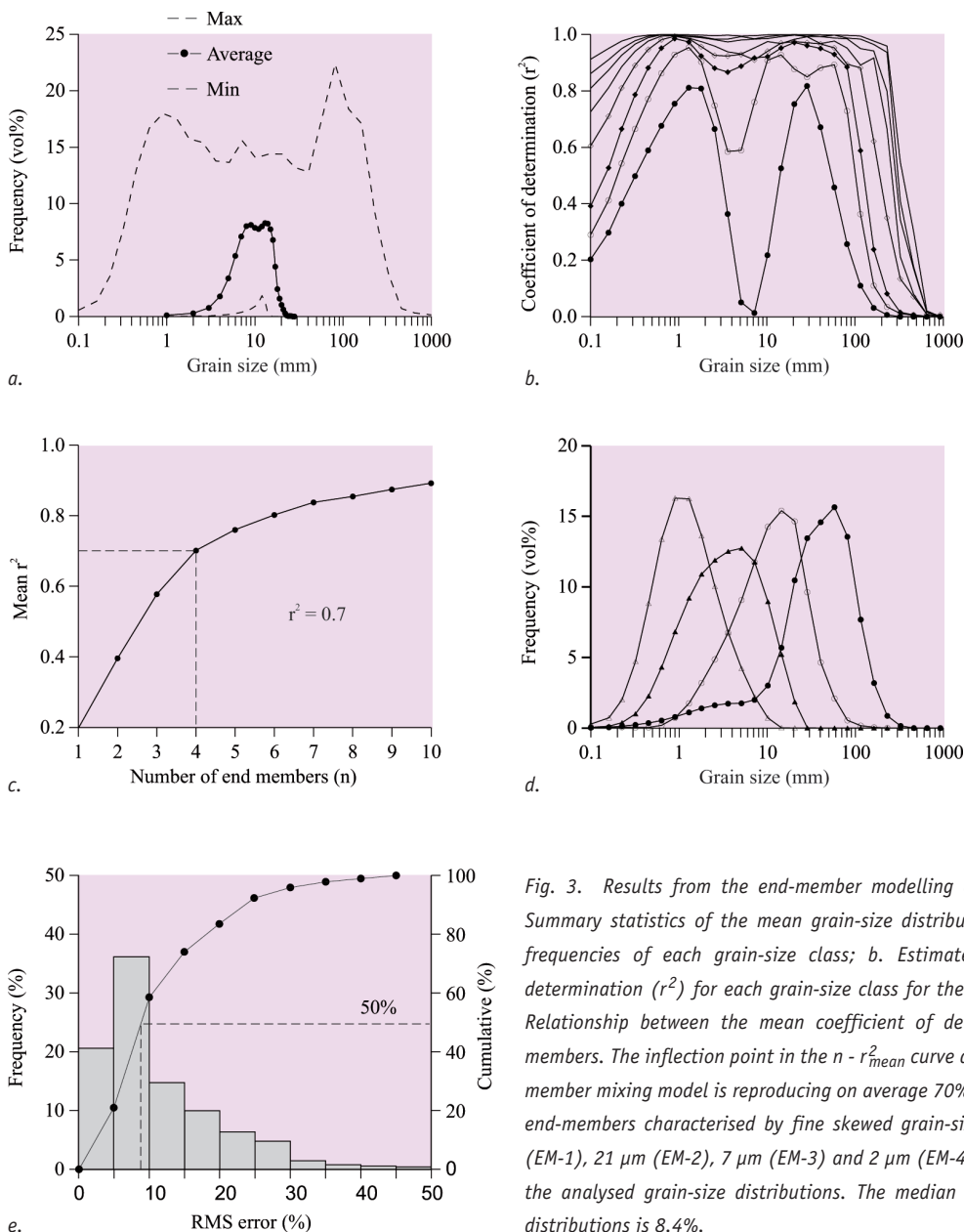

Fig. 3. Results from the end-member modelling of the sediments from core Fq-9C. a. Summary statistics of the mean grain-size distributions with maximum range of volume frequencies of each grain-size class; b. Estimated distribution of the coefficient of determination (r^2) for each grain-size class for the different numbers of end-members; c. Relationship between the mean coefficient of determination and the number of end-members. The inflection point in the $n - r^2_{mean}$ curve at n = 4 ($r^2_{mean} = 0.7$) shows a four end-member mixing model is reproducing on average 70% of the variance in the dataset; d. Four end-members characterised by fine skewed grain-size distributions with modes of 81 μm (EM-1), 21 μm (EM-2), 7 μm (EM-3) and 2 μm (EM-4); e. Root-mean square errors (RMS) of the analysed grain-size distributions. The median RMS error for the analysed grain-size distributions is 8.4%.

relative to a four-EM model. The four EMs are characterised by fine skewed to symmetrically distributed GSD and clearly defined modes of 81 µm (EM-1), 21 µm (EM-2), 7 µm (EM-3) and 2 µm (EM-4) (Fig. 3d). The ratio sand (>63 µm): coarse-silt (63-16 µm): fine-silt (16-4 µm): clay (<4 µm) is 42:44:8:6 for EM-1, 3:44:42:11 for EM-2, 0:7:46:47 for EM-3, and 0:0:14:86 for EM-4. Hence, EM-1 represents sandy sediment, EM-2 coarse silty sediment, EM-3 fine silty sediment, and EM-4 clayey sediment. The root-mean square errors (RMS) of the analysed grain-size distributions indicate how closely the analysed distributions are approximated by the four-EM mixing model. The median RMS error for the analysed grain-size distributions is 8.4% (Fig. 3e).

Based on experiments on the relationship between volume versus weight percentages (Vriend & Prins, 2005) the proportional contribution of the EMs along the record was re-scaled in proportion to LOI% of each sample. It is assumed that the EM proportions expressed by volume are similar to the EM proportions expressed by weight, and that the proportional contribution of biogenic opal (diatoms), fine dispersed volcanic ash, and carbonate to the bulk sediment is negligible (see method section). In effect, LOI is considered as an additional EM. For comparison, the initial EM proportions are also shown (Fig. 4). LOI content of the sediment varies between 1 and 88 wt%, with an average of 7 wt%. This implies that the siliciclastic fraction varies between 99 and 12 wt%, respectively, with an average of 93 wt%. High LOI values are measured in the 50.8-50.3 m composite depth (mcd) interval (up to 88 wt%), in the 32-34 mcd interval (up to 55 wt%), in the 20.7-22.5 mcd interval (up to 85 wt%), and in the 14.5-15.5 mcd interval (up to 40 wt%). The lowest LOI values are present between 8 and 10 mcd with an average value less than 2 wt%.

The aquatic pollen record is taken from Bogotá-Angel et al., (2011b). The proportional contribution of sandy sediment (EM-1), coarse silty sediment (EM-2), fine silty sediment (EM-3), clayey sediment (EM-4), and OM (peat) (based on LOI values) are compared with the downcore proportions of deep water vegetation, shallow water vegetation, cyperaceous reedswamp, and shore vegetation (Fig. 4). Biotic and abiotic signals may have independent drivers which make a combination of these proxies very effective to study basin dynamics.

Sedimentary sequences

Using CONISS we recognised nine discrete sedimentary sequences characterised by diffenrent proportional contributions of the EMs (Fig. 4; Table 1).

Sequence 9 (58.4-50.9 mcd, 284-243 ka) is dominated by clayey and fine silty sediments (EM-4 and EM-3) including the fine grained fraction of wind-blown volcanic ash. Intervals with input of sandy sediments (EM-1) are relatively small. The amount of OM is low with an average value of 3.9 wt%. Presence of deformed sedimentary structures show the sediment is affected by bioturbation.

Table 1. List of discrete sequences in record Fq-9C record from Lake Fúquene based on stratigraphically constrained cluster analysis. Characteristic values of the four end-members and the amount of organic matter, and proportions of aquatic plant categories are shown.

	Depth (m)	Age (ka)	LOI (%)	EM-1 (%)	EM-2 (%)	EM-3 (%)	EM-4 (%)
1	1.7-9.7	27-62	9.6	9.9	43.1	15.9	21.5
2	9.7-13.6	62-79	5.2	1.9	47.6	23.9	21.4
3	13.6-15.3	79-87	9.3	25.4	36.9	20.6	7.8
4	15.3-20.7	87-111	3.7	7.2	42.8	23.9	22.4
5	20.7-25.9	111-133	13.3	2.7	21.0	39.8	23.2
6	25.9-36.5	133-179	5.3	3.4	29.4	34.2	27.6
7	36.5-41.4	179-201	2.7	23.3	38.2	22.7	13.1
8	41.4-50.9	201-243	8.4	4.4	24.4	28.9	33.9
9	50.9-58.4	243-284	3.9	3.1	23.1	30.4	39.5

Sequence 8 (50.9-41.4 mcd, 243-201 ka) shows clear alternations of sandy, silty and clayey intervals. The amount of OM is correlated with presence of coarse silty and sandy sediments (EM-2 and EM-1) although not all sandy intervals are rich in OM. The lowest interval rich in OM (peat) is 60 cm thick and contains up to 88 wt% OM. This peaty interval shows intercalated laminations with coarse silty and sandy sediment (EM-2 and EM-1). The frequency of these intercalations decreases upwards while bioturbation is increasing in this direction.

Sequence 7 (41.4-36.5 mcd, 201-179 ka) is characterised by high proportions of the coarse silty and sandy end-members (EM-2 and EM-1). The sandy layers show sharp and erosive contacts at their lower boundaries. Sedimentary structures are poorly defined due to significant bioturbation and sediment density instabilities. The proportion of OM is low with an average of 2.7 wt%.

Sequence 6 (36.5-25.9 mcd, 179-133 ka) shows a variable texture with predominantly silty and clayey sediment (EM-4, EM-3 and EM-2). The lower half of this interval is characterised by high proportions of fine silt and clays, the latter in combination with relatively high proportions of OM. Sediment in the upper half of this interval is coarser with intercalations of coarse silt, and sometimes sand. Deformed structures over the sequence points to bioturbation and density instabilities.

Sequence 5 (25.9-20.7 mcd, 133-111 ka) starts with alternations of parallel laminated fine silt and clay (EM-3 and EM-4) intercalated with volcanic ash layers. Fine sediments at the lower part of this interval are changing upwards into coarse silt which finally changes into a conspicuous layer of sandy peat of 130 cm thick. During the drilling procedure over-pressured methane escaped from the peat layer disturbing its original structure.

Sequence 4 (20.7-15.3 mcd, 111-87 ka) is characterised by coarse silty sediments (EM-2) and low contents of OM. Most sediment structures are affected by bioturbation.
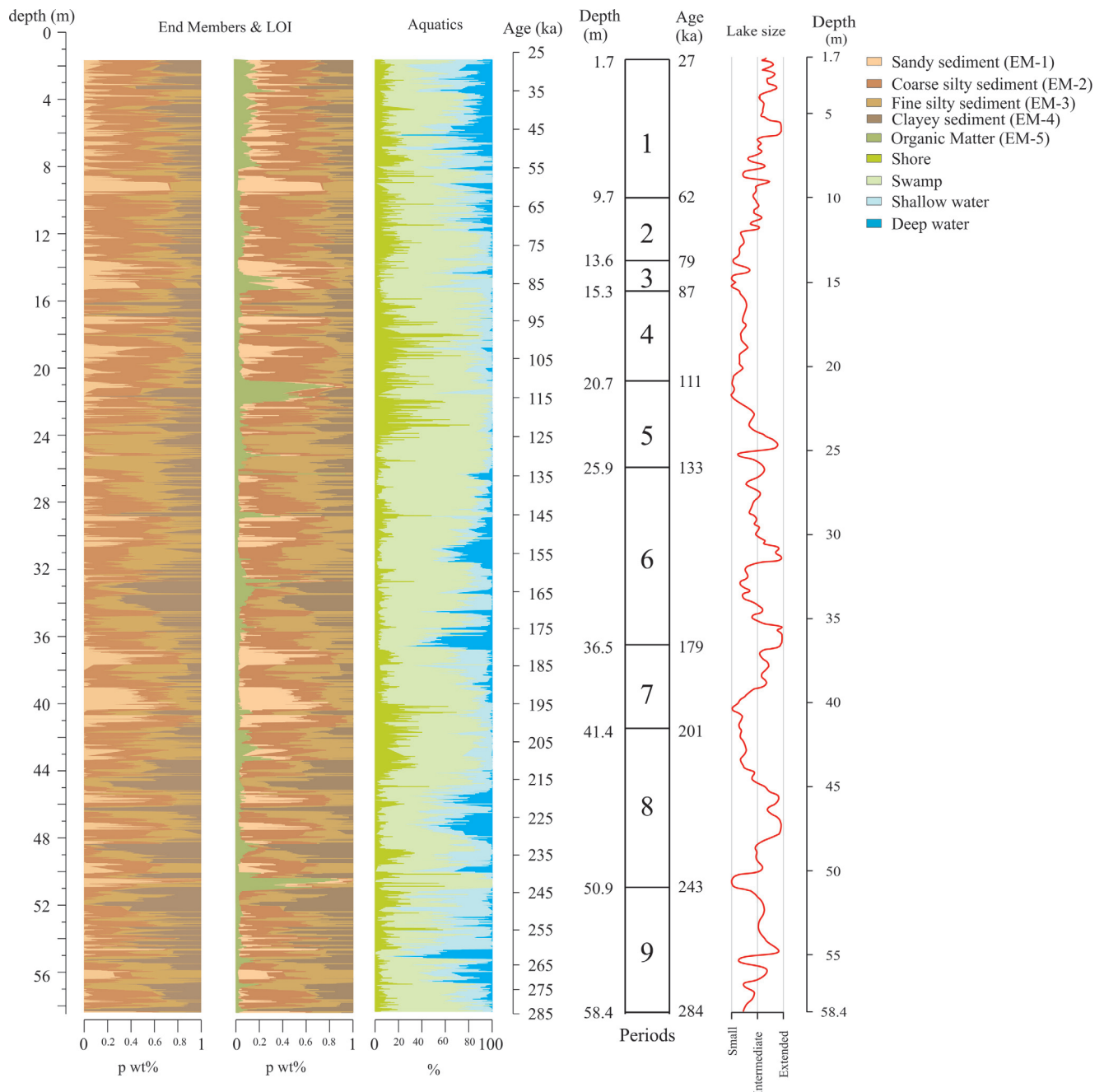
Fig. 4. *Left: downcore proportions of four end-members produced by the End Member Model Algorithm (EMMA). Centre: downcore proportions of five end-members: EM-1 (sandy sediments) to EM-4 (clayey sediments) were produced by EMMA, and EM-5 (organic matter and peat) has been developed from the loss-on-ignition data (see explanation in the text). Right: downcore proportions of four categories of aquatic plants ranging from shore vegetation (left) to deep water vegetation (right). The red curve shows the inferred lake level record.*

Sequence 3 (15.3-13.6 mcd, 87-79 ka) is characterised by sandy sediment (EM-1). The lower half of this interval is rich in OM. Marks produced by vegetation and bioturbation are clearly visible in the OM rich sediments.

Sequence 2 (13.6-9.7 mcd, 79-62 ka) is characterised by high proportions of coarse silty sediment (EM-2) and low proportions of sandy sediment (EM-1). The coarse silty sediments are intercalated with layers of laminated fine silt and clay and in the sedimentary structures there is clear evidence of bioturbation.

Sequence 1 (9.7-1.7 mcd, 62-27 ka) is characterised by high proportions of coarse silty sediment (EM-2), frequently alternating with sandy intervals (EM-1); the lowest sandy layer is half a metre thick. The proportion of fine silty sediment is relatively low while the proportion of the clayey sediment is comparable with the preceding sequence. The amount of OM is relatively high with an average value of 11 wt%.

Genetic interpretation of the modelled sediment components

The modal grain sizes in the range from clay to fine-sand represent different transport and depositional processes. The sediment particles represented by EM-2, EM-3 and EM-4 are likely transported into the lake as suspended load. The finest clay particles (EM-4) stay in permanent suspension as long as some water flow is present. High proportions of EM-3 and EM-4 in the sediments likely indicate that the drilling site was distally located relative to the sediment source pointing to a large lake size. The relative coarse particles of EM-1 are transported to the lake as bedload or in turbidity currents, depending on flow velocity. The sandy layers in the lake sediments generally show eroded lower boundaries without evidence of cross-bedding or ripples. This suggests that the least particles of EM-1 are deposited with significant energy by sediment-laden currents. Such currents may be derived directly from rivers during floods or from episodic slumps due to sediment instability in the fan area in the lake. The low topographical gradients in the basin makes it unlikely that such currents travel for long distances. High proportions of EM-1 therefore, probably indicate that the drilling site is proximally located relative to the sediment source pointing to a small lake size. Previous studies of north Andean lakes showed small lake sizes generally coincide with periods of relatively high temperatures (Van 't Veer & Hooghiemstra, 2000; Torres et al., 2005). Following this line of reasoning, high proportions of EM-2, EM-3 and EM-4, indicating that the drilling site was distally located relative to the sediment source, points to a large lake size in combination with relatively low (glacial/stadial) temperatures. We considered LOI values as an additional EM (EM-5) and we rescaled the proportional contribution of EM-1 to EM-4. OM accumulates in particular in shallow water or under swampy conditions. Therefore, a high proportion of EM-5 is indicative of a swampy environment with abundant stagnant water near the drilling site.

The degree of complexity of the sedimentation processes is schematically illustrated (Fig. 5) by the observation that the four-end-member model is explaining 'only' 70% of the observed variance in the grain-size data. In addition, the RMS error is relatively high with a median of 8.4 % (Fig. 3e). For comparison, Chinese loess records are well described as mixtures of three aeolian dust components explaining 81-87% of the observed variance in the grain-size data, with a median RMS error ranging from 1.2 to 4.5% (Vriend & Prins, 2005; Prins et al., 2007; Prins & Vriend, 2007; Vriend et al., 2011). Here size distributions of coarse sediments are less well approximated than size distributions of finer sediments. This suggests that EM-1 reflect most variable sedimentation processes. Inspection of the total grain size dataset reveals that coarse sediment samples show very similar distribution spectra which show only variation in the modal grain size (which can be as high as 230 µ). In contrast, modal grain sizes in the fine sand fraction (125-250 µm) are scarce.

Lake size fluctuations

Based on visual inspection of the sediments Sarmiento et al. (2008) provided an initial reconstruction of lake-level changes from core Fq-9C. The presence of OM in the sediments was used as an indication of high production of plant biomass pointing to shallow water, or swampy conditions. The impact of vegetation and microfauna on the lake floor was expected to decrease with rising water levels, resulting in diminished bioturbation. Therefore, presence of OM and the degree of bioturbation was the main evidence for their initial reconstruction. There is no evidence of pedogenic processes indicating that Lake Fúquene never desiccated for a significant length of time. At this centrally located site sediments did not accumulate any more after 27 ka or were not preserved. At the borders of the lake sediment accumulation continues up to the present (Bogotá-Angel et al., 2011b) suggesting this centrally located site suffered from streamline erosion.

The flatness of the basin floor allows the lake border to migrate significantly when lake-level change is in the order of several decimetres (Fig. 6). Therefore changing water budgets in the catchment area will have more impact on lake size rather than on water depth. Hence, changes in lake size likely have influenced the GSD of the sediments accumulated at the drilling site. The strength of the multi-proxy approach is that aquatic pollen is informative of water depth, while GSD is indicative of the distance to the source area of the sediments and/or the general level of available energy in the catchment area. In this paper, the proportional contribution of EMs (Fig. 4,
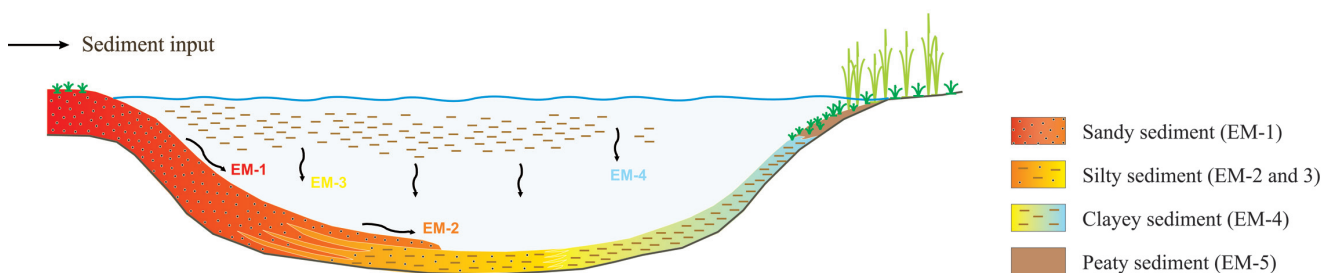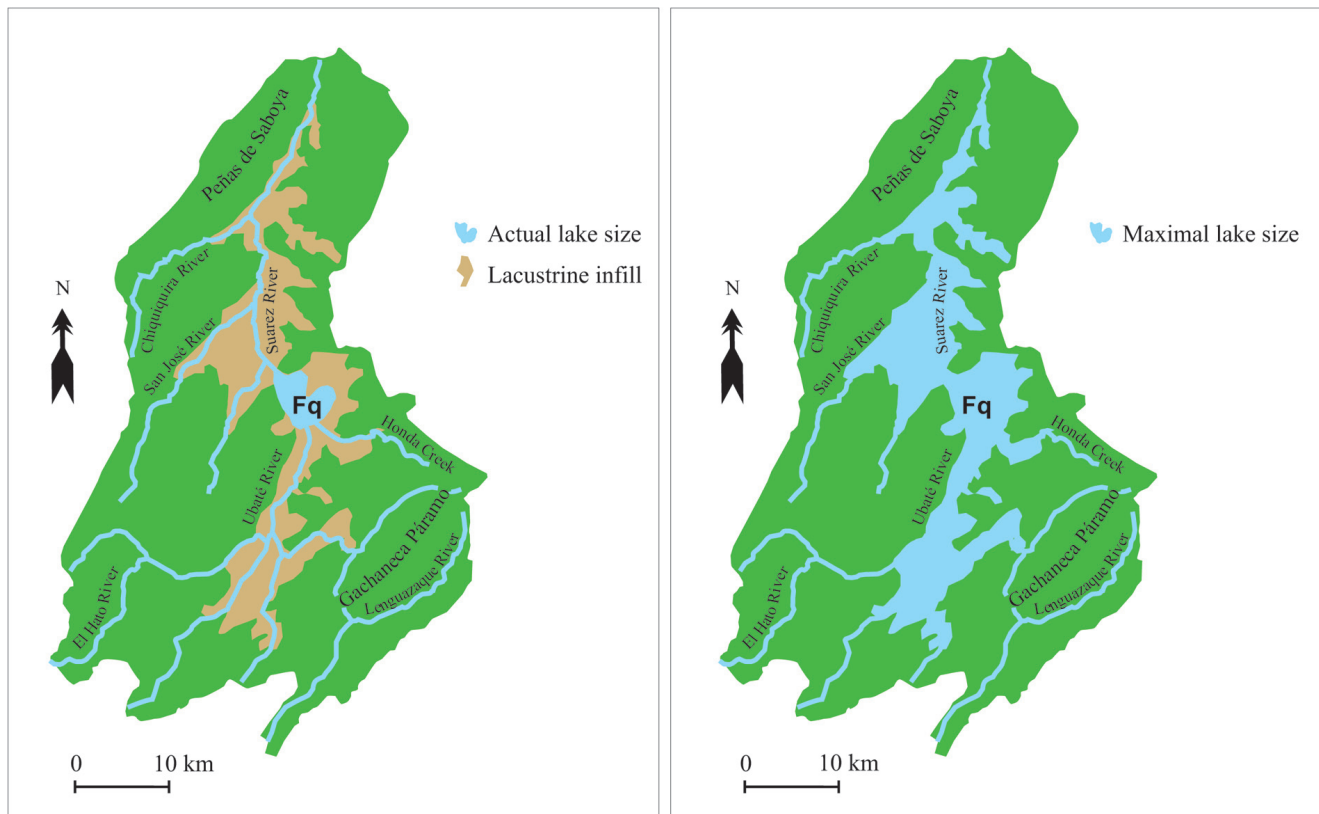

Fig. 5. Schematic cross-section through Lake Fúquene showing the relationship of four distinct sediment populations with modal grain sizes in the range from clay (EM-1) to fine-sand (EM-4) to the distance to the sediment source area.

a.   b.

Fig. 6. Visualisation of the surface area of Lake Fúquene. a. A small lake size occurred during relatively warm periods when levels of evaporation are relatively high (reflects the present-day setting); b. A large lake size occurred during relatively cool and cold periods when levels of evaporation are relatively low. The floor of the Fúquene Basin is totally covered by the water body. (With permission after unpublished material from S. Gaviria and G. Sarmiento, Bogotá).

left hand panel), the proportion of peat and OM rich sediments based on LOI values (Fig. 4, central panel), and aquatic vegetation (Fig. 4, right hand panel) were combined to reconstruct lake size fluctuations. A large lake is characterised by relatively high proportions of deep water vegetation, low proportions of shore vegetation, and high proportions of fine silty and clayey sediment (EM-3 and EM-4). A small lake is characterised by high proportions of swamp and shore vegetation, low proportions of deep water vegetation, and proximal sediment input prevails. However, proximal sediment input with a low water budget in the basin may supply significant proportions of fine grained sediments (EM-3 and EM-4), while proximal sediment input with a high water budget in the basin may supply high proportions of sandy and coarse silty sediment (EM-1 and EM-2). High LOI values reflect presence of peaty layers, indicative of shallow water.

Relationships between GSD, lake size, and net evaporation can be complicated by changing sediment budgets due to vegetation cover, or melting glaciers. During interglacial conditions the catchment area was covered by dense vegetation preventing significant erosion by rain splash and overland flow. Therefore, small quantities of coarse grained sediments will be transported to the lake suggesting a large

sized lake. High proportions of coarse sediments, potentially related to episodes of melting glaciers (Helmens et al., 1997) may cause an underestimation of the size of the lake.

Characteristic lacustrine depositional environments

Here biotic and abiotic proxy information is synthesised and four discrete depositional environments are distinguished based on the proportional contribution of the five EMs, the proportional contribution of four categories of aquatics, and reconstructed water depth. The location of site Fq-9C relative to the sediment source and the type of depositional environment is shown in block diagrams (Fig. 7) and representative core intervals are shown (Fig. 8).

Fig. 7a shows a large sized lake with an accumulation of predominantly fine sediments (EM-4 and EM-3). Sedimentation of clayey and fine silty sediment occurs in standing water or under conditions of slow water motions. In interval 56.20-54.00 mcd deep water and shallow water aquatics are abundant and represent open water conditions (Fig. 8a). Low arboreal pollen (AP) values show mainly cold climatic conditions. Spikes of sandy intervals (EM-1) are frequent. Abundant fine silt (EM-3) in the lower part coincides with presence of shallow water
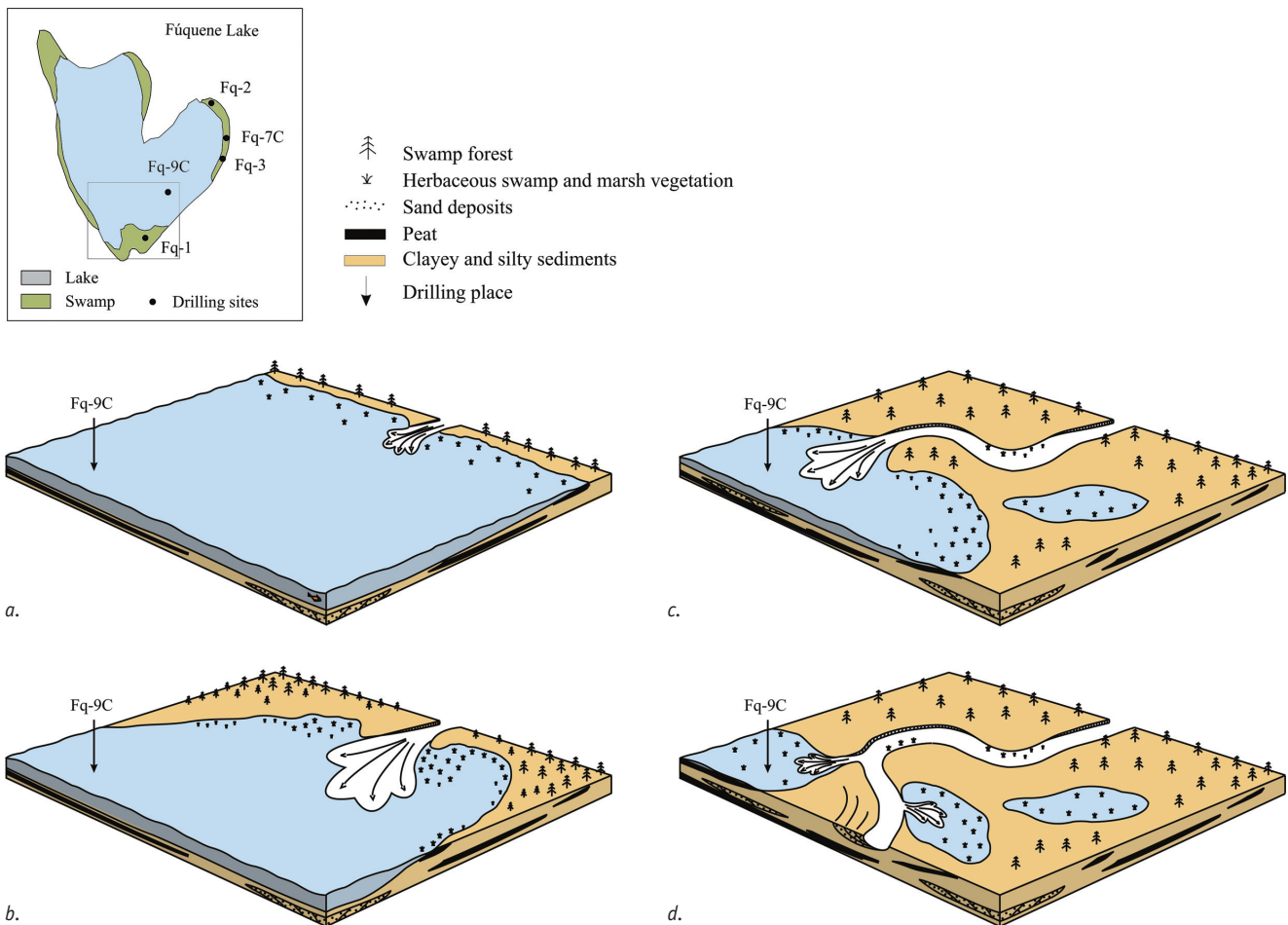
Fig. 7. Schematic block diagrams showing the setting of depositional environments with (a) large lake size / distal sediment source in particular facilitating deposition of clayey and fine silty sediment (EM-4 and EM-3); (b) intermediate lake size in particular facilitating deposition of fine silty and course silty sediment (EM-3 and EM-2); (c) small lake size / proximal sediment source in particular facilitating deposition of course silty and sandy sediment (EM-2 and EM-1); (d) swamp environment / proximal source area in particular facilitating deposition of organic rich silty sediment (EM-3 and EM-2), sandy sediment (EM-1) and peat. Figures adapted after Torres et al. (2005) with permission.

(middle panel) and high representation of cool subpáramo vegetation. Abundant clay (EM-4) in the upper part coincides with deeper water, lower temperatures and presence of grasspáramo around the lake. Significant presence of OM and peat (EM-5) coincides with most shallow water conditions and highest temperatures (highest AP% values).

Fig. 7b shows a depositional environment with an intermediate lake size. The coring site is regularly influenced by currents set up by river inflows interrupting accumulation of the finest clayey sediment (EM-4). Distal river inlets result in fine and coarse silty sediment (EM-3 and EM-2) at the coring site. In interval 4.30-2.30 mcd (Fig. 8b) intermediate lake sizes are reflected (middle panel). Higher AP% values show cool climatic conditions. There is a trend of increasing cold páramo vegetation, first replacing *Polylepis* dwarf forest near the UFL and later replacing Andean forest. Lowering temperatures (right panel) coincide with increasing deep water environments (middle panel) and increasing proportions of finest sediments (EM-4 and EM-3). OM and peat is continuously abundant and

coincides with peaks of sand (EM-1), fine silt (EM-2), as well as coarse silt (EM-3). This suggests abundant peat is most related to absence of cold conditions but may coincide with various energy levels and distances to sediment sources.

Fig. 7c shows a depositional environment in a small lake. Decreasing lake size may cause lacustrine deltaic flats prograding over the finer prodelta deposits towards the coring site. Proximal river inflow and even turbidity-like currents may dominate the sedimentary transport and deposition processes, resulting in accumulation of predominantly coarse sediments (EM-3, EM-2 and EM-1). Interval 53.00-50.20 mcd (Fig. 8c) shows a decreasing lake size (middle panel) which coincides with increasing temperatures (right panel) culminating in a period with extensive presence of peatland. Shallow water conditions coincide with coarse silt (EM-2), fine silt (EM<-3) as well as with clay (EM-4). Higher proportions of fine silt coincides with abundant subpáramo vegetation and intermediate temperatures, while higher proportions of clay coincides with abundant grasspáramo and lower temperatures and deeper water. Spikes
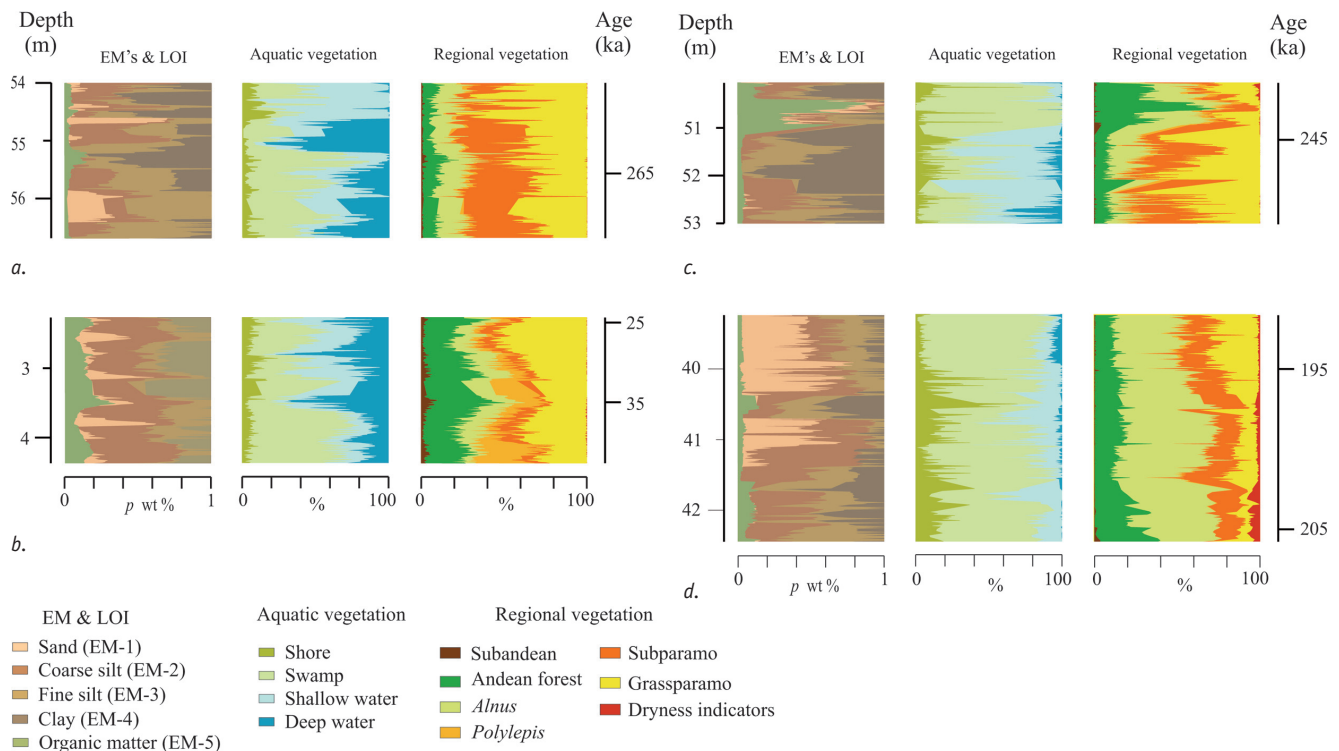
Fig. 8. *Selected intervals of record Fq-9C of Lake Fúquene showing four characteristic depositional environments in terms of grain size distributions (left hand panel) and aquatic pollen spectra (central panel). The right hand panel shows downcore proportions of altitudinally organised biomes (subandean forest at lowest elevations; grasspáramo at highest elevations) and selected individual trees (Alnus: below the upper forest line, Polylepis: around and above the upper forest line). The altitudinally shifting forest/páramo boundary (= upper forest line) reflects changes in mean annual temperature (forest = subandean trees, Andean trees, and Alnus). a. large lake size; b. intermediate lake size c. small lake; and d. swampy environment (see explanation in the text).*

of sand (EM-1) systematically coincide with presence of peat. We interpret this combination of indicators of contrasting energy levels as evidence that peatland along the border of a lake was filtering and accumulating coarse sediments.

Fig. 7d shows a swampy environment with accumulation of predominantly OM and presence of peat at the drilling site. Considering the relatively high proportions of EM-1 and EM-2 siliciclastic sediments are deposited by stream spill or lateral stream migration. Interval 42.45-39.30 mcd (Fig. 8d) shows swampy environments (middle panel) under high interglacial temperatures (right panel). Abundant dry vegetation in the lower part of this interval (right panel) coincides with absence of deep water vegetation and absence/lowest proportions of sand (EM-1). These relationships are plausible when available precipitation and energy levels to transport sediments is considered. Two times proportions of OM and peat increased substantially coinciding with an increase of clay (EM-4) but not coinciding with presence of sand as was the case in Figs. 7c and 8c. Here climatic conditions were drier and sediments in the basin were transported at a lower energetic level.

Relationships lake depth, lake size, sediment source, precipitation, energy level of the drainage system, rate of erosion, presence of OM, abundance of peat, and the abundance of sand, coarse silt, fine silt and clay are summarised (Fig. 9). During glacial conditions the proportion of exposed rock and uncovered
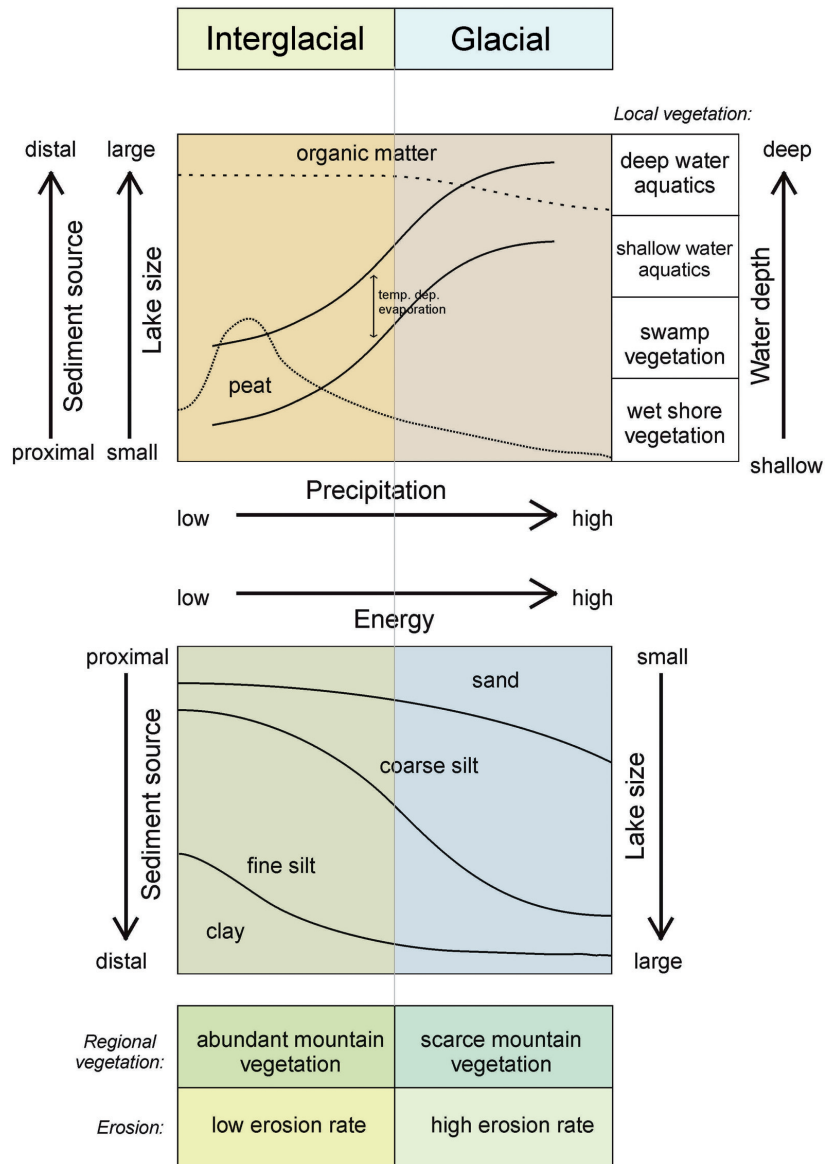
soils in the drainage basin was high while during interglacial conditions most of the drainage basin was covered by forest. Most of the record fits this idealised description but alternative settings occur. For example coarse silt and sand is most abundant when source areas are proximal, precipitation and erosion is abundant, and energy levels are high. But peatland at the border of the lake may serve as a filter resulting in the combination of sand and peat, both sediment fractions characteristic of contrasting environmental conditions.

Reconstruction of lacustrine environments and discussion

Here we integrate the information from the various proxies for the nine discrete core intervals (Fig. 4) with focus on specific depositional environments, sediment transport, sediment accumulation processes, and lake size and water depth. Climatic conditions are related to the global marine isotope stages (MIS) of the $\partial^{18}O$ record (Imbrie et al. 1984)

The period from 284 to 243 ka, representing most of MIS-8, shows significant proportions of swamp and shallow water vegetation pointing to intermediate lake sizes most of the time. Clayey sediment occurs frequently often associated with presence of OM pointing to standing water. From 280 to 250 ka five discrete peaks of sandy and coarse silty sediments coincide

Fig. 9. Idealised relationships between the biotic and abiotic basin environments and climate-controlled precipitation-erosion-energy dynamics. Left hand parts of both panels show warm (interglacial) settings; right hand parts show cool to cold glacial settings. Top panel shows relationships between precipitation, water depth (and related dominant aquatic vegetation, and lake size), abundance of organic matter including peat, and distance to the source area of the sediments. During warm interglacial conditions peat is more abundant while during cool and cold glacial conditions plant biomass develops mainly into amorph organic matter. Lake levels are systematically higher during interglacial/interstadial conditions and the difference between the two curves is explained by higher evaporation under higher temperatures. Bottom panel shows relationships between energy level (and related sediment source and lake size) and abundance of four grain size fractions. Abundant vegetation cover in the drainage basin under warmer conditions prevents easy erosion and transport resulting in higher proportions of peat and fine-grained sediments than during cool to cold climatic conditions (After Hooghiemstra, unpublished data).

with an increase of shallow and deep water vegetation, while clay and fine silty sediments in between these peaks coincide with more abundant shore and swamp vegetation.

The period from 243 to 201 ka, representing most of MIS-7, shows abundant sediments with high levels of OM. At the start (243-239 ka) extensive peatlands were present and peat is mixed up with little sand and fine silt while the vegetation consisted of swamp and wet shore vegetation. After the interval with peat, the sequence shows significant proportions of sand and sandy silt, however three times interrupted (around 234 ka, 223 ka, and 217-211 ka) by a period with abundant fine silt and clay. These interruptions occurred when swamp vegetation was abundant reflecting low lake levels (at 234 ka and 217-211 ka) but also when abundant shallow and deep water aquatics indicate high water levels (223 ka). From 205-210 ka there was another sandy peat interval (low lake level) and up to the end of this sequence fine silt and clay is increasing while shallow water plants diminished and swamp vegetation expanded.

The period from 201 to 179 ka, representing the transition from MIS 7 to MIS 6, shows three intervals with high proportions of sand and sandy silt (200-198 ka, 196-192 ka and 185-180 ka). The first two intervals coincide with abundant swamp and lake shore vegetation (low water levels) while the third coarse grained interval coincides with a higher water level and a larger lake size. The trend during this sequence is an expanding lake and an increasing abundance of clay and fine silty sediment; this trend seems characteristic at a transition from interglacial to glacial conditions.

The period from 179 to 133 ka, representing most of MIS 6, starts with a deep water setting and large lake (179-177 ka) while coarse and fine silts are dominant. The remaining part of this sequence shows a lower lake level (177-158 ka) with abundant fine silt, clay, and OM under mainly swampy conditions; an interval (158-153 ka) with almost exclusively fine and course silt under conditions of an increasing water depth; and an upper interval (153-133 ka) with decreasing

proportions of sandy silt, increasing proportions of fine silt and clay, expansion of swampy area, and low water level conditions.

The period from 133 to 111 ka, representing MIS 5e, shows successively three different settings. The period of 134-125 ka is dominated by fine silty sediment with presence of clay and peat while swampy conditions prevailed. The interval 125-116 ka shows similar proportions of coarse silt and fine silt, while proportions of clay and peat do not change, and swampy conditions continued. The interval 116-111 ka shows extensive peatlands for the second time in this record (the first peatlands occurred from 243 ka to 239 ka) but now with clay and in absence of sand. Water levels were low and the lake size was small.

The period from 111 to 87 ka, representing MIS 5d to 5b, shows two characteristic settings. From 111 ka to 94 ka coarse silt and sand show highest proportions with a continuous presence of organic material while wet shore vegetation and swamp was abundant pointing to low water level. From 94 ka to 90 ka high proportions of fine silt and clay, and dominance of swamp and lake shore vegetation point to low lake levels with an almost absence of coarse sediment input. From 90 ka to 87 ka input of coarse silt increased and the proportion of clay diminished while swampy conditions continued to prevail.

The period from 87 to 79 ka, representing most of MIS 5a, shows a continuous input of sandy sediments. In the first part in combination with abundant OM (period 87-83 ka) while swamp vegetation dominated, and in the last part with lower proportions of OM and higher proportions of coarse silt while shallow water conditions increased.

The period from 79 to 62 ka, representing most of MIS 4, shows a large proportion of coarse silt, with some spikes of sandy input and an almost constant input of OM. The proportion of swamp and wet shore vegetation was high and the decreasing trend in its abundance reflects the decreasing proportion of OM in the sediments which coincides with higher water levels in the lake.

The period from 62 to 27 ka, representing most of MIS 3, starts with a significant input of sand from 62 ka to 59 ka. There was a change from swampy conditions to shallow water and the lake reached deeper water after 50 ka. Periodically there is significant input of sand and coarse silt alternating with input of fine silt and clay. Periodic input of sand coincides with episodic increases of the water level.

Comparison of sediment records from the Bogotá and Fúquene basins

A visual comparison between records of GSD and aquatic pollen was first made by Torres et al. (2005) in core Funza-2 from the adjacent Bogotá Basin. They showed a record of lake level change, identification of eleven facies in four distinct depositional environments with different accumulation rates, sedimentation discontinuities, and records of vegetation change. In the present Fq-9C record we used the EMMA

algorithm to obtain grain size classes and we added a category representing 'organic rich sediments and/or peat'. The presence of peat in the lithological column mainly coincided with presence of Andean forest around the lake. Also under modern conditions peat growth in high Andean lakes is mainly restricted to elevations below the UFL (Cleef & Hooghiemstra, 1984).

Temporal changes in the lithology and grain size distribution are more frequent in Lake Fúquene (this paper) as is the case in paleo-lake Bogotá (Torres et al., 2005). In both basins cores were drilled at centrally located sites. Both lakes were during the period recorded fed by many small streams from the surrounding slopes and both have a relatively small river serving as water input (Bogotá River, and the Ubaté River, respectively) and water output (Bogotá River, and Suarez River, respectively). Palaeo-lake Bogotá deposited lacustrine sediments up to ~50 m above the altitude of the present lake floor (Van der Hammen & González, 1960; Hooghiemstra, 1984) while Lake Fúquene deposited lacustrine sediments up to ~20 m above the present-day lake level. These values are indicative of the maximum lake-levels during Pleistocene time. The average sediment accumulation in both lakes is similar: ~47 yr/cm in paleo-lake Bogotá (based on core Funza-2; Torres et al., unpublished data) versus ~45 yr/cm in Lake Fúquene (based on record Fq-9C; Groot et al., 2011). Both lakes differ in average size (we estimate that during the same period of time paleo-lake Bogotá was approximately two times larger than Lake Fúquene), shape (the Fúquene Basin is elongated and narrow while the Bogotá Basin is mainly isodiametric and the lake may have grown to a surface of ~40 × 60 km), proximity to the sediment sources (site Fq-9C is more proximal than site Funza-2), and available energy to transport sediments to the coring sites (depositional settings of site Fq-9C resemble more Fig. 7c-7d, while depositional settings at site Fuza-2 resemble more Fig. 7b-7a). Considering all together, record Fq-9C shows changes in the dynamic abiotic and biotic environment with most expression. Previous observations that in a large lake regional changes are better reflected while in a smaller lake local changes are more precisely monitored (Jacobson & Bradshaw, 1981; Prentice, 1985; Sugita, 1993; Weng et al., 2006 and the references therein) are substantiated.

Conclusions

We applied the EMMA algorithm to a 4768 point time series of GSDs of lacustrine sediments that span with ~60 yr resolution the period from 284 ka to 27 ka. We showed that four EMs explains an optimal proportion (70%) of the observed variation in GSDs. EMMA is able to unmix GSDs of lacustrine sediments in a genetically meaningful way. This means that sediment categories (EMs) can be interpreted as depositional and environmental settings of the past. Most unexplained variability is located in the coarse sediment fraction. GSDs only measure

the minerogenic part of sediments as a standard. A fifth EM reflecting the abundance of OM was developed on the basis of LOI data. Palaeo-environmental reconstructions reached a high detail by integrating information from abiotic and biotic proxies. We recognised four categories of grain size distributions (clayey, fine silty, coarse silty, and sandy sediments) reflecting environments from standing water to turbidite currents. The location of the sediment source in relation to the drilling site (proximal to distal) and available level of energy to transport sediments in the catchment area was established. We recognised four categories of aquatic plants which are characteristic of wet shores, swamps, shallow water, and deep water conditions. These categories reflect a hydrological gradient which is sensitive for water level changes. Finally we placed the dynamic history of changes in the aquatic vegetation, sediment transport, and sedimentary environments in the basin in the context of climatic change. Groot et al. (2011) showed from this record climate change at submillennial time scales and this variability is also reflected in the changing sedimentary environment. In general, relatively warm (interglacial) to mild (interstadial) periods coincide with relatively low lake level stands while relatively cold (glacial) to cool (stadial) periods coincide with relatively high lake level stands. We assume higher evaporation during these relatively warm intervals explains this relationship. Further analysis of this data set is challenging to explore relationships between proxies shown in Fig. 7 as well as to address changes in sediment accumulation in between tie points of the age model.

References

Battarbee, R.W., 1986. Diatom analysis. *In:* Berglund, B.E. (ed.): Handbook of Holocene palaeoecology and palaeohydrology. Wiley, New York: 527-570.

Beaudoin, A., 2003. A comparison of two methods for estimating the organic content of sediments. Journal of Paleolimnology 29: 387-390.

Bogotá-Angel, R.G., Gaviria, S., Rincón-Martínez, D., Sarmiento, G., Hooghiemstra, H., Berrio, J.C., Groot, M.H.M., Verstraten, J.M. & Jansen, B., 2011a. Geochemical basin dynamics related to its sedimentary, vegtational and climate histories: a case study from the Fúquene Basin, northern Colombian Andes. *In:* Bogotá-Angel, R.G.: Pleistocene centennial-scale vegetational, environmental, and climatic change in the Colombian Andes. PhD thesis, University of Amsterdam: 105-126.

Bogotá-Angel, R.G., Groot, M.H.M., Hooghiemstra, H., Lourens, L.J., Van der Linden, M. & Berrio, J.C., 2011b. Rapid climate change from North Andean Lake Fúquene pollen records driven by obliquity: implications for a basin-wide biostratigraphic zonation. Quaternary Science Reviews 30: 3321-3337.

Bogotá-Angel, R.G., Hooghiemstra, H. & Berrio, J.C., 2011c. An ultra-high resolution multi-proxy record from Lake Fúquene (Colombia); orbital to submillennial-scale dynamics of montane vegetation, climate, lake-level changes and sedimentary environments, I: period 284-130 kyr before present. *In:* Bogotá-Angel, R.G.: Pleistocene centennial-scale vegetational, environmental, and climatic change in the Colombian Andes. PhD thesis, University of Amsterdam: 49-97.

Burrough, S.L., Thomas, D.S.G., Shaw, P.A. & Bailey, R.M., 2007. Multiphase Quaternary highstands in Lake Ngami, Kalahari, northern Botswana. Palaeogeography Palaeoclimatology Palaeoecology 253: 280-299.

CAR, 2000. Fúquene; el lecho de la zorra. Corporación Autónoma Regional de Cundinamarca (Bogotá), Colombia, 189 pp.

CAR, 2002. Atlas ambiental CAR 2001 (1st ed. 2002). Corporación Autónoma Regional de Cundinamarca, Bogotá, Colombia, 175 pp.

Chaparro, B., 2003. Reseña de la vegetación en los humedales de la Sabana de Bogotá. *In:* Conservation International – Colombia, Los humedales de Bogotá y la Sabana, Vol. 1. Panamericana (Bogotá), Colombia: 71-89.

Chapron, E., Juvigné, E., Mulsow, S., Ariztegui, D., Magand, O., Bertrand, S., Pino, M. & Chapron, O., 2007. Recent clastic sedimentation processes in Lake Puyehue (Chilean Lake District, 40.5° S). Sedimentary Geology 201: 365-385.

Cleef, A.M., 1981. The vegetation of the páramos of the Colombian Cordillera Oriental. Dissertationes Botanicae 61. J. Cramer (Vaduz), 320 pp.

Cleef, A.M. & Hooghiemstra, H., 1984. Present vegetation of the area of the high plain of Bogotá. *In:* Hooghiemstra, H. (ed.): Vegetational and climatic history of the high plain of Bogotá, Colombia. Dissertationes Botanicae 79. J. Cramer, (Vaduz): 42-66.

Cortés, S.P. & Rangel-Ch., J.O., 2000. Los relictios de vegetación en la Sabana de Bogotá. *In:* Aguirre, J. (ed.): Memorias del Primer Congreso Colombiano de Botánica (Bogotá), Colombia, versión en CD-Rom.

Cuatrecasas, J., 1958. Aspectos de la vegetación natural de Colombia. Revista de la Academia Colombiana Ciencias Exactas Fisicas y Naturales 10 (40): 221-264.

Feagri, K. & Iversen, J., 1989. Text book of pollen analysis. 4th ed. Wiley (Chichester).

Gill, D. Shomrony, A. & Fligelman, H., 1993. Numerical zonation of log suites and log facies recognition by multivariate clustering. The American Association of Petroleum Geologist Bulletin 77: 1781-1791.

Grabandt, R.A.J., 1980. Pollen rain in relation to arboreal vegetation in the Colombian Cordillera Oriental. Review of Palaeobotany and Palynology 29: 65-147.

Grimm, E.C., 1987. CONISS: A Fortran 77 program for stratigraphically constrained cluster analysis by the method of the incremental sum of squares. Computer and Geosciences 13: 13-35.

Groot, M.H.M., Hooghiemstra, H., Berrio, J.C., Giraldo-P, C. & Vriend, M., in review. An ultra-high resolution multi-proxy record from Lake Fúquene (Colombia); orbital to submillennial-scale dynamics of montane vegetation, climate, lake-level changes and sedimentary environments, II: period 130-27 kyr before present.

Groot, M.H.M., Bogotá, R.G., Lourens, L.J., Hooghiemstra, H., Vriend, M., Berrio, J.C., Tuenter, E., Van der Plicht, J., Van Geel, B., Ziegler, M., Weber, S.L. & Fúquene project Members, 2011. Ultra-high-resolution pollen record from the northern Andes reveals rapid shifts in montane climates within the last two glacial cycles. Climate of the Past 7: 299-316.

Grubb, P.J., 1974. Factors controlling the distribution of forest-types on tropical mountains. *In:* Flenley, J.R. (ed.): Altitudinal zonation in Malesia. Transactions Third Aberdeen-Hull Symposium on Malesian Ecology, University of Hull, Dept. of Geogr., Miscellaneous Series No. 16: 13-45.

Helmens, K.F., Rutter, N.W. & Kuhry, P., 1997. Glacier fluctuations in the Eastern Andes of Colombia (South America) during the last 45,000 radiocarbon years. Quaternary International 38/39: 39-48.

Holz, C., Stuut, J.B.W. & Henrich, R., 2004. Terrigenous sedimentation processes along the continental margin of NW Africa: implications from grain-size analysis of seabed sediments. Sedimentology 51: 1145-1154.

Holz, C., Stuut, J.B.W., Rüdiger, H. & Meggers, H., 2007. Variability in terrigenous sedimentation processes off northwest Africa and its relation to climate changes: Inferences from grain-size distributions of a Holocene marine sediment record. Sedimentary Geology 202: 499-508.

Hooghiemstra, H., 1984. Vegetational and climatic history of the high plain of Bogotá, Colombia. Dissertationes Botanicae 79. J. Cramer, Vaduz, 368 pp.

Hooghiemstra, H., Wijninga, V.M. & Cleef, A.M., 2006. The paleobotanical record of Colombia: implications for biogeography and biodiversity. Annals Missouri Botanical Garden 93: 297-324.

IGAC, 2003. Atlas de Colombia; 5th edition 2002. Instituto Geografico Agustin Codazzi, Bogotá D.E., Colombia.

Imbrie, J., Hays, J.D., Martinson, D.G., McIntyre, A., Mix, A.C., Morley, J.J., Pisias, N.G., Prell, W.L. & Shackleton, N.J., 1984. The orbital theory of Pleistocene climate: support from a revised chronology of the marine $\partial^{18}O$ record. *In:* Berger, A., Imbrie, J., Hays, J., Kukla, G. & Saltzman, B. (eds): Milankovitch and climate, Part 1. NATO ASI Series C 126. Reidel (Dordrecht), the Netherlands: 269-305.

Ingeominas, 1991. Mapa geológico de Colombia. Instituto de Investigaciones en Geociencias, Minería y Química (Bogotá) Colombia.

Jansen, J.H.F., Van der Gaast, S.J., Koster, B. & Vaars, A.J., 1998. COTEX, a shipboard XRF-scanner for element analysis in split sediment cores. Marine Geology 151: 143-153.

Julià, R. & Luque, J.A., 2006. Climatic changes vs. catastrophic events in lacustrine systems: A geochemical approach. Quaternary International 158: 162-171.

Konert, M. & Vandenberghe, J., 1997. Comparison of laser grain size analysis with pipette and sieve analysis: a solution for the underestimation of the clay fraction. Sedimentology 44: 523-535.

Lisiecki, E.L. & Raymo, M.E., 2005. A Pliocene-Pleistocene stack of 57 globally distributed benthic $\partial^{18}O$ records. Paleoceanography 20, PA1003.

Mommersteeg, H., 1998. Vegetation development and cyclic and abrupt climatic change during the Late Quaternary. PhD thesis, University of Amsterdam, 191 pp.

Prentice, I.C., 1985. Pollen representation, source area, and basin size: toward a unified theory of pollen analysis. Quaternary Research 23: 76-86.

Prins, M.A., Vriend, M., 2007. Glacial and interglacial eolian dust dispersal patterns across the Chinese Loess Plateau inferred from decomposed loess grain-size records. Geochemistry Geophysics Geosystems 8.Q07/Q05.doi 10.1029/2006GC001563.

Prins, M.A. & Weltje, G.J., 1999a, End-member modelling of grain-size distributions of sediment mixtures. *In:* Prins, M.A.: Pelagic, hemipelagic and turbidite deposition in the Arabian Sea during the late Quaternary: Unravelling the signals of aeolian and fluvial sediment supply as functions of tectonics, sea-level and climate change by means of end-member modelling of siliciclastic grain-size distributions. Geologica Ultraiectina 168, PhD thesis, University of Utrecht: 47-68.

Prins, M.A. & Weltje, G.J., 1999b, End-member modeling of siliciclastic grain-size distributions: The late Quaternary record of aeolian and fluvial sediment supply to the Arabian Sea and its paleoclimatic significance. *In:* Harbaugh, J., et al. (eds): Numerical experiments in stratigraphy: Recent advances in stratigraphic and sedimentologic computer simulations, SEPM (Society for Sedimentary Geology) Special Publication 62: 91-111.

Prins, M.A., Postma, G. & Weltje, G.J., 2000. Controls on terrigenous sediment supply to the Arabian Sea during the late Quaternary: the Makran continental slope. Marine Geology 169: 351-371.

Prins, M.A., Bouwer, L.M., Beets, C.J., Troelstra, S.R., Weltje, G.J., Kruk, R.W., Kuijpers, A. & Vroon, P.Z., 2002. Ocean circulation and iceberg discharge in the glacial North Atlantic: inferences from unmixing of sediment distributions. Geology 30: 555-558.

Prins, M.A., Vriend, M., Nugteren, G., Vandenberghe, J., Lu, H., Zheng, H. & Weltje, G.J, 2007. Late Quaternary aeolian dust input variability on the Chinese Loess Plateau: inferences from unmixing of loess grain-size records. Quaternary Science Reviews 26: 242-254.

Rangel-Ch., J.O., 2003. El antiguo lago de la Sabana de Bogotá su vegetación y su flora en el tiempo. *In:* Los humedales de Bogotá y la sabana. Empresa de Acueducto, Agua y Alcantarillado de Bogotá, Conservación Internacional: 53-70.

Rangel Ch., J.O. & Aguirre-C., J., 1983. Comunidades acuáticas altoandinas I. Vegetación sumergida y de ribera en el Lago de Tota, Boyacá, Colombia. Caldasia 13: 719-742.

Rangel Ch., J.O. & Aguirre-C., J., 1986. Estudios ecológicos en la Cordillera Oriental Colombiana, III. La vegetación de la cuenca del Lago de Tota (Boyacá). Caldasia 15: 263-311.

Riezebos, P.A., 1978. Petrographic aspects of a sequence of Quaternary volcanic ashes from the Laguna de Fúquene area, Colombia, and their stratigraphic significance. Quaternary Research 10: 401-424.

Santos-Molano, E. & Guerra-C., C., 2000. Fúquene; el lecho de la zorra. Corporación Autónoma Regional de Cundinamarca (CAR) (Bogotá), Colombia, 189 pp.

Sarmiento, G., Gaviria, S., Hooghiemstra, H., Berrio, J.C. & Van der Hammen, T., 2008. Landscape evolution and origin of Lake Fúquene (Colombia): tectonics, erosion and sedimentation processes during the Pleistocene. Geomorphology 100, 563-575.

Stuut, J.B.W., Prins, M.A., Schneider, R.S., Weltje, G.J., Jansen, J.H.F. & Postma, G., 2002. A 300 kyr record of aridity and wind strength in southwestern Africa: evidence from grain-size distributions of sediments on Walvis Ridge, SE Atlantic. Marine Geology 180: 221-233.

Stuut, J-B.W. & Lamy, F., 2004. Climate variability at the southern boundaries of the Namib (southwestern Africa) and Atacama (northern Chile) coastal deserts during the last 120,000 yr. Quaternary Research 62: 301-309.

Sugita, S., 1993. A model of pollen source area for an entire lake surface. Quaternary Research 39: 239-244.

Torres, V., Vandenberghe, J. & Hooghiemstra, H., 2005. An environmental reconstruction of the sediment infill of the Bogotá basin (Colombia) during the last 3 million years from abiotic and biotic proxies. Palaeogeography Palaeoclimatology Palaeoecology 226: 127-148.

Torres, V., 2006. Pliocene-Pleistocene evolution of flora, vegetation and climate: a palynological study of a 586-m core from the Bogotá Basin, Colombia. Unpublished PhD thesis, Univ. Amsterdam, the , 181 pp.

Van der Hammen, T., 1974. The Pleistocene changes of vegetation and climate in tropical South America. Journal of Biogeography 1: 3-26.

Van der Hammen, T. & González, E., 1960. Upper Pleistocene and Holocene climate and vegetation of the Sabana de Bogotá (Colombia, South America). Leidse Geologische Mededelingen 25: 126-315.

Van der Hammen, T. & Hooghiemstra, H., 2003. Interglacial-glacial Fúquene-3 pollen record from Colombia: an Eemian to Holocene climate record. Global and Planetary Change 36: 181-199.

Van Geel, B. & Van der Hammen, T., 1973. Upper Quaternary vegetational and climatic sequence of the Fúquene area (Eastern Cordillera, Colombia). Palaeogeography Palaeoclimatology Palaeoecology 14: 9-92.

Van 't Veer, R. & Hooghiemstra, H., 2000. Montane forest evolution during the last 650 000 yr in Colombia: a multivariate apptoach based on pollen record Funza-1. Journal of Quaternary Science 15: 329-346.

Vriend, M. & Prins, M.A., 2005. Calibration of modelled mixing patterns in loess grain-size distributions: an example from the north-eastern margin of the Tibetan Plateau, China. Sedimentology 52: 1361-1374.

Vriend, M., Prins, M.A., Buylaert, J.-P., Vandenberghe, J. & Lu, H., 2011. Contrasting dust supply patterns across the north-western Chinese Loess Plateau during the last glacial-interglacial cycle. Quaternary International, doi: 10.1016/j.quaint.2010.11.009.

Weltje, G.J., 1997. End-member modelling of compositional data: numerical-statistical algorithms for solving the explicit mixing problem. Journal of Mathematical Geology 29: 503-549.

Weltje, G.J. & Prins, M.A., 2003. Muddled or mixed? Inferring paleoclimate from size distributions of deep-sea clastics. Sedimentary Geology 162: 39-62.

Weltje, G.J. & Prins, M.A., 2007. Genetically meaningful decomposition of grain-size distributions. Sedimentary Geology 202: 409-424.

Wolin, J.A. & Duthie, H.C., 1999. Diatoms as indicators of water level change in fresh water lakes. *In:* Stoermer, E.F. & Smol, J.P. (eds.): The diatoms: applications for the environmental and earth sciences. Cambridge University Press (Cambridge), U.K.: 183-202.